Weld-Bottom Macrosegregation Caused by Dissimilar Filler Metals

Filler metals with a large difference in liquidus temperature from the base metal can cause severe macrosegregation, and mechanisms are proposed to explain this

BY Y. K. YANG AND S. KOU

ABSTRACT. Filler metals different (dissimilar) from the base metal in composition are common in arc welding, but macrosegregation can exist in the resultant welds and degrade the weld quality. Two macrosegregation mechanisms (Mechanisms 1 and 2) have been proposed recently for the case of complete mixing between the filler metal and the bulk weld pool. Here the case of incomplete mixing was investigated. The liquidus temperatures of the bulk weld metal T_{LW}, base metal T_{LB}, filler metal T_{LF}, and partially mixed filler metal near the pool bottom $T_{LF'}$ were considered in addition to the stagnant or laminar-flow layer of liquid base metal along the weld pool boundary suggested by Savage. Mechanism 3 is for filler metals making $T_{LW} < T_{LB}$ and thus $T_{LF} < T_{LF'} < T_{LW} < T_{LB}$. The partially mixed filler metal solidifies into a filler-rich zone near the pool bottom with a solidification front at $T_{LF'}$. Since $T_{LF'}$ is well below T_{LB}, there exists ahead of the front a wide region cooler than T_{LB}. Thus, convection can easily carry the liquid base metal from the layer into the cooler region to freeze quickly before complete mixing occurs. This results in a partially mixed base metal in a filler-rich zone near the weld bottom. The binary Ni-Cu alloy system was chosen because large differences in liquidus temperatures can be selected to clearly verify the mechanisms. Ni was welded by gas metal arc welding (GMAW) with filler metal Cu. A filler-rich zone existed as proposed, with islands of partially mixed base metal scattered near the weld bottom. Evidence of quick freezing was found. Mechanism 4 is for filler metals making $T_{LW} > T_{LB}$ and thus $T_{LF} > T_{LF'} > T_{LW} > T_{LB}$. The partially mixed filler metal freezes quickly in the region cooler than $T_{LF'}$ near the pool bottom. This results in a filler-rich zone near the weld bottom that intrudes into a filler-deficient beach along the fusion boundary. Cu was welded with filler metal Ni. A filler-rich zone and a filler-deficient beach existed as proposed. Evidence of quick freezing was again found. With filler metal Cu-30Ni, macrosegregation was similar but less.

Y. K. YANG and S. KOU (skou@wisc.edu) *are, respectively, graduate student and professor in the Department of Materials Science and Engineering, University of Wisconsin, Madison, Wis.*

Introduction

Dissimilar filler metals, that is, filler metals different from the workpiece in composition, are routinely used in arc welding. It has been recognized for more than 40 years that macrosegregation can exist near the fusion boundary of arc welds made with dissimilar filler metals and degrade the weld quality (Refs. 1–17). The present study deals with welding one workpiece material with a dissimilar filler metal, that is, dissimilar-filler welding, and the resultant weld is called a dissimilar-filler weld. Welding two metals of different compositions together with or without a filler metal, that is, dissimilar-metal welding, is beyond the scope of the present study.

Kou and Yang (Refs. 18, 19) have recently studied macrosegregation near the fusion boundary of dissimilar-filler welds. The filler metal mixed completely with the homogeneous bulk weld pool and macrosegregation was caused by poor mixing of the liquid base metal with the bulk weld pool alone. The liquidus temperature of the bulk weld metal T_{LW} and the liquidus temperature of the base metal T_{LB} were considered in addition to the stagnant or laminar-flow layer of liquid base metal along the weld pool boundary suggested by Savage (Ref. 3).

KEYWORDS

Dissimilar Filler Metals
Macrosegregation
Solidification
Weld Pool
Liquidus Temperature
Ni-Cu
Filler-Rich Zone

Kou and Yang (Ref. 18) presented the following fundamental solidification concepts for dissimilar-filler welding, which can also be applied to the present study. First, the melting front is at T_{LB} instead of T_{LW}, because solid-state diffusion is far too slow to change the composition of the solid to that in equilibrium with the bulk weld metal to make it melt completely at T_{LW}. Second, the solidification front is no longer isothermal everywhere at T_{LW} as in welding without a dissimilar filler metal (undercooling is assumed negligible in most arc welding). It is at T_{LW} only along the bulk solidification front where the homogeneous bulk weld pool begins to solidify at its liquidus temperature T_{LW}. Third, the liquid base metal can freeze quickly in a liquid cooler than T_{LB} before complete mixing occurs, so can the liquid weld metal freeze quickly in a liquid cooler than T_{LW}. Either way, macrosegregation is promoted. Fourth, if the filler metal makes $T_{LW} < T_{LB}$, complete mixing throughout the weld pool may be possible under ideal conditions, but if the filler metal makes $T_{LW} > T_{LB}$, complete mixing is impossible because the base metal along the outside of the boundary of complete mixing is still above T_{LB} and thus must form a liquid layer of the base metal.

Macrosegregation can occur near the fusion boundary even when the filler metal mixes completely with the bulk weld pool. In light of the solidification concepts described above, Kou and Yang (Ref. 18) proposed two mechanisms for such macrosegregation. In Mechanism 1, for filler metals making $T_{LW} < T_{LB}$, the region of liquid weld metal immediately ahead of the bulk solidification front (T_{LW}) is below T_{LB} simply because of $T_{LW} < T_{LB}$ and not any undercooling. The liquid base metal swept in here from the liquid base-metal layer by convection can freeze quickly into filler-deficient penin-

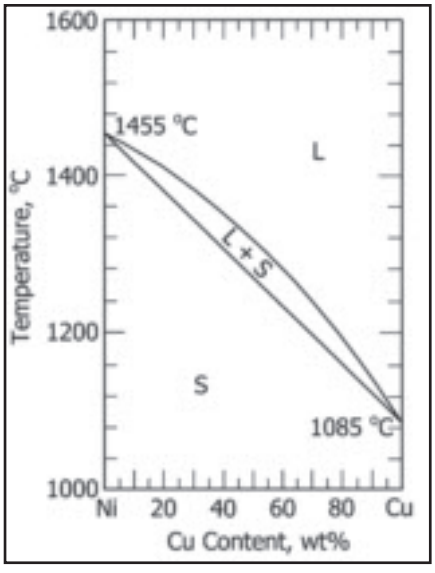

Fig. 1 — Ni-Cu phase diagram (Ref. 21).

sulas or islands. These peninsulas or islands often appear roughly parallel to the fusion boundary in a weld transverse or longitudinal micrograph. The liquid base metal remaining in the layer solidifies as a filler-deficient beach. This mechanism was confirmed by macrosegregation in gas metal arc welds of 1100 Al (essentially pure Al) made with filler metal 4145 Al (essentially Al-4Cu-10Si), which made $T_{LW} < T_{LB}$.

In Mechanism 2, for filler metals making $T_{LW} > T_{LB}$, the stagnant or laminar-flow layer of liquid base metal is below T_{LW} simply because $T_{LW} > T_{LB}$. The liquid weld metal pushed in here from the bulk weld pool by convection can freeze quickly as weld-metal intrusions into an often continuous filler-deficient beach. Meanwhile, the liquid base metal left in the space between the intrusions can solidify into filler-deficient peninsulas or islands of random orientations. These filler-deficient features are distinctly different from those formed by Mechanism 1. This was a new kind of macrosegregation not reported previously. This mechanism was confirmed by macrosegregation in gas metal arc welds of Cu made with filler metal Cu-30Ni, which made $T_{LW} > T_{LB}$.

The present study focuses on the macrosegregation that forms in the weld when the dissimilar filler metal reaches the weld pool bottom before it is completely mixed with the bulk weld pool. Two mechanisms, Mechanisms 3 and 4, are proposed to explain such macrosegregation. These two mechanisms are more complicated than Mechanisms 1 and 2 described previously for the macrosegregation that forms near the fusion boundary when the dissimilar filler metal is completely mixed with the bulk weld pool. The binary Ni-Cu alloy system is selected as a test material. Macrosegregation in these welds differs significantly both in morphology and severity from that observed previously near the fusion boundary (Ref. 18).

The binary Ni-Cu alloy system is selected for welding because of the following reasons. First, as will be shown later (in Fig. 1), it has a simple phase diagram easy for understanding the weld microstructure. Second, it has a wide temperature range over which T_{LW} and T_{LB} can be varied relative to each other. A large difference between T_{LW} and T_{LB} will make its effect on macrosegregation more signifi-

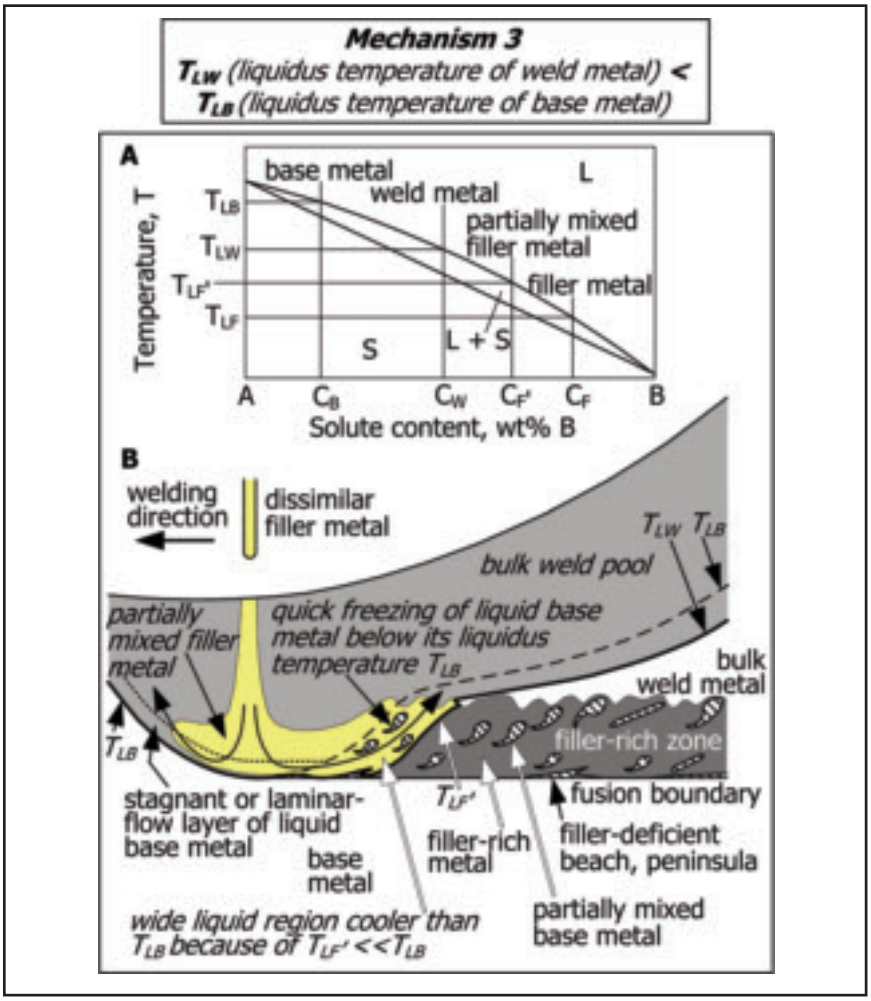

Fig. 2 — Mechanism for macrosegregation formation caused by a partially mixed dissimilar filler metal that makes $T_{LW} < T_{LB}$ (Mechanism 3). A — Phase diagram; B — longitudinal cross section of weld pool.

Table 1 — Welds, Dilutions, Compositions, and Liquidus Temperatures

		Composition (wt-%)			Liquidus Temperature (°C)			
Welds	Dilution	Base Metal (b)	Filler Metal (f)	Weld Metal	Base Metal (T_{LB})	Filler Metal (T_{LF})	Weld Metal (T_{LW})	$\Delta T = T_{LB} - T_{LW}$ (°C)
Ni(b)/Cu(f)	51.4%	Ni > 99.0	Cu > 99.99	Cu-51.3Ni	1455	1085	1321	+134
Ni(b)/Cu-30Ni(f)	38.9%	Ni	Cu-30.4Ni	Cu-57.4Ni	1455	1239	1342	+113
Cu(b)/Ni(f)-1	35.3%	Cu > 99.99	Ni > 99.67	Cu-64.7Ni	1085	1455	1366	–281
Cu(b)/Ni(f)-2	44.1%	Cu	Ni	Cu-55.9Ni	1085	1455	1338	–253
Cu(b)/Cu-30Ni(f)	49.1%	Cu	Cu-30.4Ni	Cu-15.3Ni	1085	1239	1168	–83

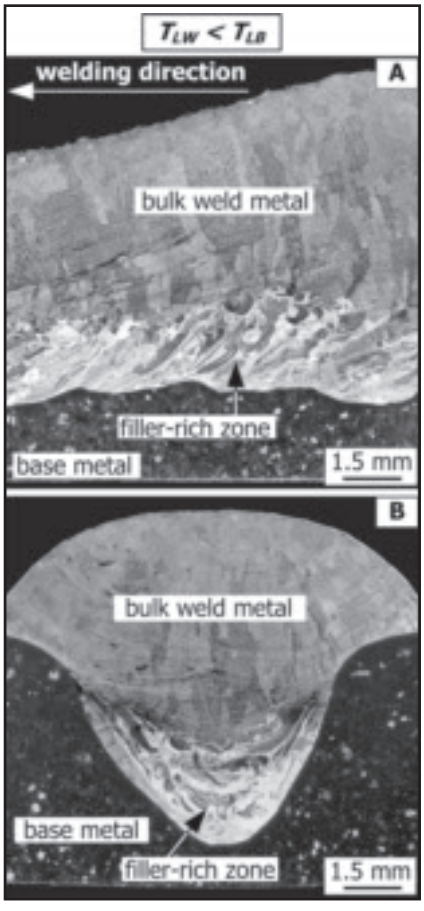

Fig. 3 — Macrographs of filler-rich zone when $T_{LW} < T_{LB}$. A — Longitudinal; B — transverse. Base metal: Ni; filler metal: Cu.

Fig. 4 — Longitudinal micrograph showing filler-rich zone with islands of partially mixed base metal in filler-rich metal when $T_{LW} < T_{LB}$. Base metal: Ni; filler metal: Cu.

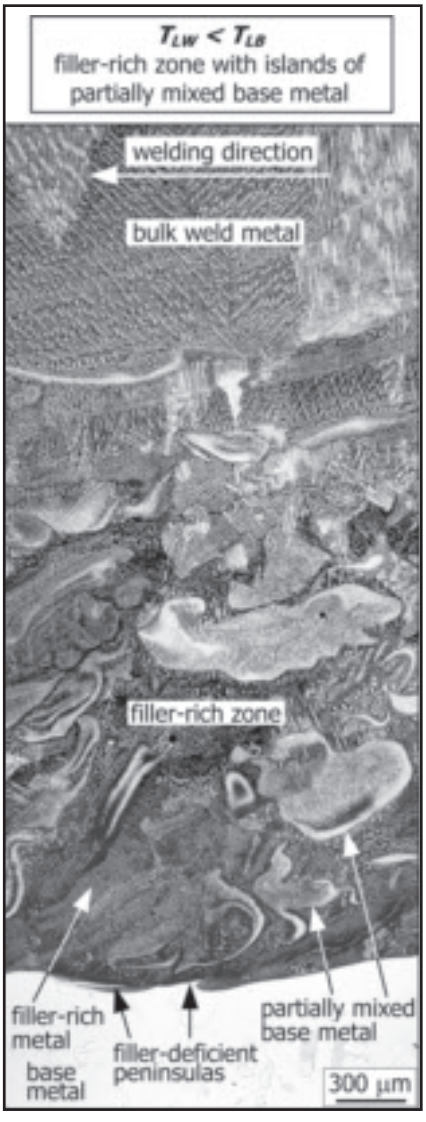

Fig. 5 — Longitudinal micrograph showing filler-rich zone with islands of partially mixed base metal in filler-rich metal and filler-deficient peninsulas along fusion boundary when $T_{LW} < T_{LB}$. Base metal: Ni; filler metal: Cu.

cant and thus easier to verify. Third, Ni and Cu are soluble in each other completely, and there are no intermetallic compounds either to complicate the weld microstructure or cause weld cracking. Fourth, welding wires or Ni, Cu, and Cu-Ni alloys (such as Cu-30Ni) are commercially available.

Experimental Procedure

Ni 200 (commercially pure Ni, 99.6% purity) and Cu 101 (also known as oxygen-free, electronic-grade Cu, 99.99% purity) were used for welding. They were all 6.4 mm (¼ in.) thick, 51 mm (2 in.) wide, and 102 mm (4 in.) long. The copper plates were heat-treated at 800°C for 24 h under argon atmosphere and cleaned before welding. This was found to improve penetration. Pure Ni, pure Cu, and Cu-30.40Ni welding wires were used. The wire diameters were 1.1, 1.3, and 1.1 mm, respectively.

Bead-on-plate gas metal arc welding (GMAW) was carried out under the following welding conditions: 6.4–8.5 mm/s (15–20 in./min) travel speed, 169 and 212 mm/s (400, 500 in./min) wire feeding rate, 30–37 V arc voltage, 300–350 A average current, and Ar shielding. The contact tube to workpiece distance was about 19 mm (¾ in.), and the torch was held perpendicular to the workpiece. The weld length on the Ni plate was about 97 mm long. As for the weld on a Cu plate, a Cu run-on plate about 75 mm long was used, allowing an extra weld length of about 25 mm on the run-on plate.

The resultant welds were cut in the middle and polished to prepare longitudinal and transverse cross sections. In some cases, in order to help reveal the development of macrosegregation, an additional longitudinal cross section was taken to include the weld crater. The samples were etched with two different etching solutions. The first etching solution was an iron chloride solution consisting of 3 g of $FeCl_3$, 2 mL of 37% HCl, and 100 mL of methanol. The second was an ammonium persulfate solution consisting of 10 g of $(NH_4)_2S_2O_8$ and 100 mL of distilled water. Welds made on pure copper were etched with the first solution to highlight the filler-rich intrusions, and then etched again with the second solution to reveal the fusion boundary in copper more clearly. All other welds were etched with the first solution only.

The concentration of any element, E, in a homogeneous weld metal can be calculated as follows (Ref. 20):

% E in weld metal = (% E in base metal)

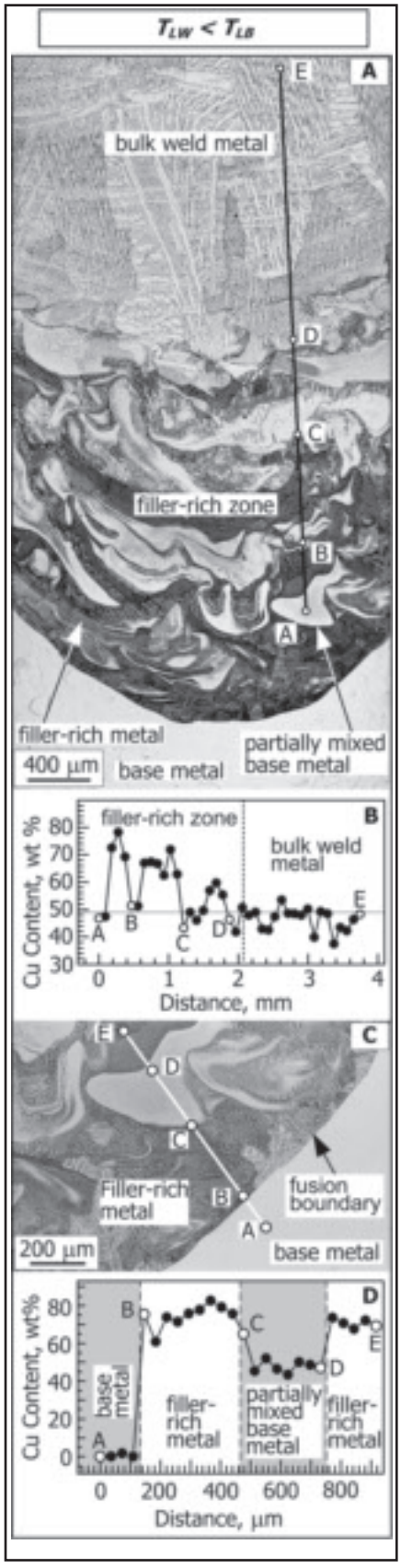

Fig. 6 — Macrosegregation in weld with $T_{LW} < T_{LB}$. A — Transverse micrograph; B — composition profile; C — transverse micrograph near fusion boundary; D — composition profile across fusion boundary. Base metal: Ni; filler metal: Cu.

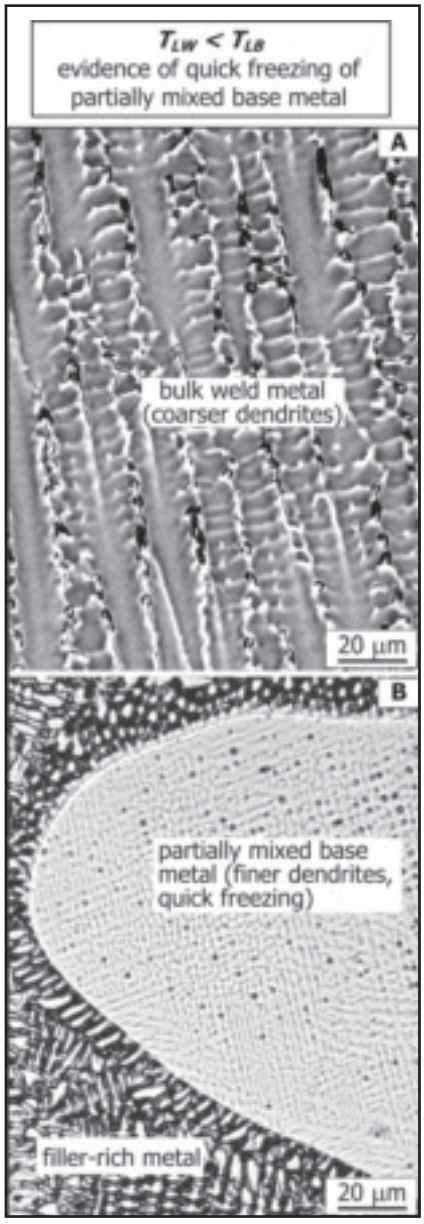

Fig. 7 — Evidence of quick freezing of partially mixed liquid base metal suggested by Mechanism 3. A — Bulk weld metal showing coarser dendrites near point E in Fig. 6A; B — left side of island at point A in Fig. 6A showing much finer dendrites than bulk weld metal. Both have about the same composition of Ni-48Cu. Base metal: Ni; filler metal: Cu.

$\times [A_b / (A_b + A_f)] + (\%\ E \text{ in filler metal}) \times [A_f / (A_b + A_f)]$ (1)

where A_b and A_f are the areas in the weld transverse cross section that are below and above the workpiece surface, respectively. Equation 1 is based on the assumption of uniform composition in the weld metal, that is, no macrosegregation (Ref. 20). Although macrosegregation was severe in the present study, it was essentially limited to near the weld bottom. Arc welds are typically much narrower at the bottom than at the top, and those in the present study were no exceptions. Thus, the volume within which macrosegregation occurred was still much smaller than the overall volume of the weld, and Equation 1 was still used as an approximation for calculating the average composition of the weld metal. Since the density of Ni (8.90 g/cm^3) is almost identical to that of Cu (8.96 g/cm^3), the accuracy of Equation 1 will not be affected by the concentrations of Ni and Cu relative to each other in the weld metal.

In Equation 1, areas A_b and A_f represent contributions from the base metal and filler metal, respectively. The ratio $A_b / (A_b + A_f)$ is the so-called dilution ratio. Areas A_b and A_f were determined by enlarging the transverse macrograph on a computer monitor and by using commercial computer software.

The welds were also examined under a scanning electron microscope, and the composition profiles across the fusion boundary were determined by energy dispersive spectroscopy (EDS).

Results and Discussion

Table 1 summarizes the results of welding experiments. For convenience, each weld is identified with the base metal (b) followed by the filler metal (f). For instance, weld Ni(b)/Cu(f) refers to a weld with pure Ni as the base metal and pure Cu as the filler metal. Similarly, weld Cu(b)/Cu-30Ni(f) refers to a weld with pure Cu as the base metal and Cu-30Ni as the filler metal.

Figure 1 shows the binary Ni-Cu phase diagram (Ref. 21). For pure Ni the liquidus temperature is its melting point 1455°C. Likewise, for pure Cu the liquidus temperature is its melting point 1085°C.

Welds with $T_{LW} < T_{LB}$

Two mechanisms are proposed as follows for macrosegregation in welds made with a dissimilar filler metal that is not completely mixed with the bulk weld pool when it reaches the pool bottom. Mechanism 3, shown in Fig. 2, is for filler metals making $T_{LW} < T_{LB}$. A phase diagram similar to the binary Ni-Cu phase diagram is shown in Fig. 2A for convenience of discussion. The composition of the base metal is C_B and that of the filler metal C_F. The composition of the resultant bulk weld metal is somewhere between C_B and C_F, depending on the extent the filler metal is diluted by the liquid base metal. The liquidus temperature of the bulk weld metal T_{LW} is below that of the base metal T_{LB}. The partially mixed filler metal near the pool bottom may not be exactly uniform in composition. As will be shown subsequently, the composition of the partially mixed filler metal C_F, is close to C_F

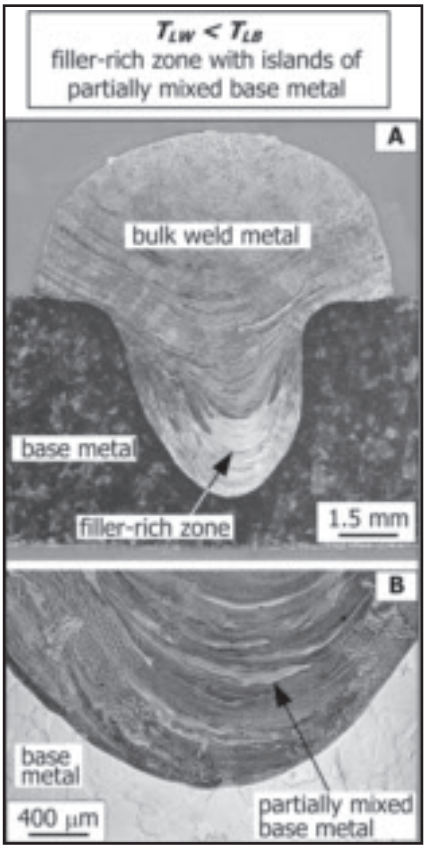

Fig. 8 — Transverse cross section of filler-rich zone formed when $T_{LW} < T_{LB}$. A — Macrograph; B — micrograph. Base metal: Ni; filler metal: Cu-30Ni.

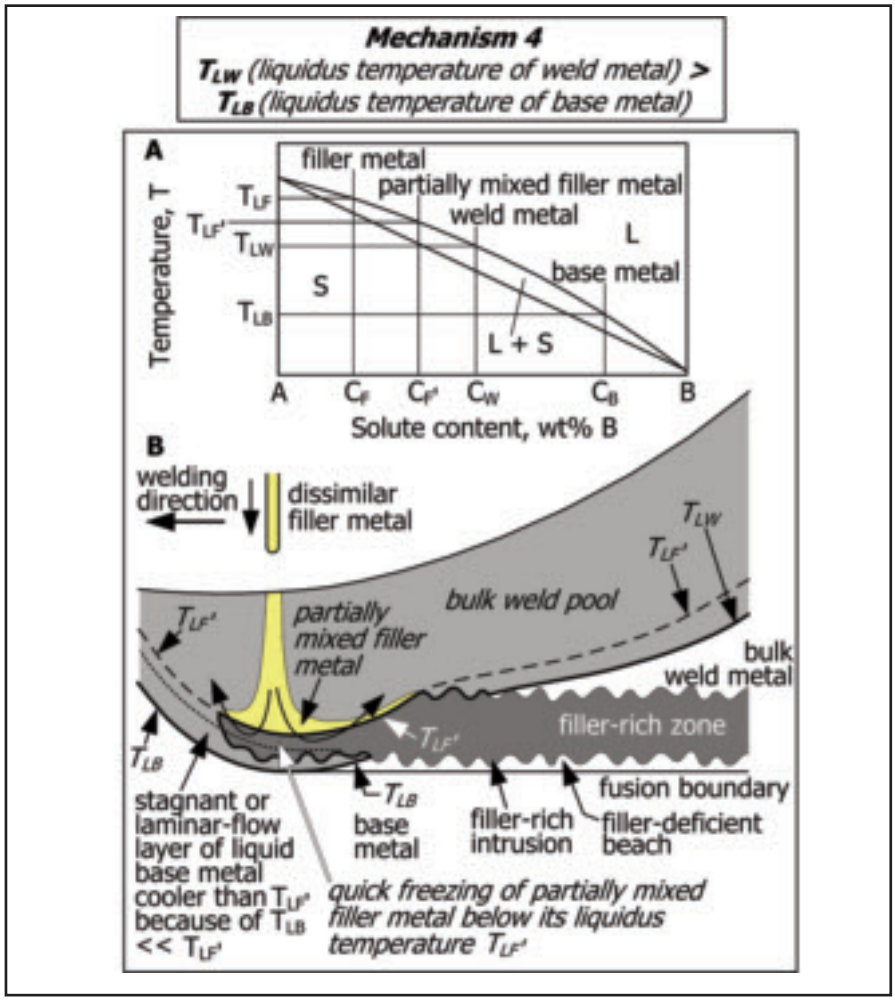

Fig. 9 — Mechanism for macrosegregation formation caused by a partially mixed dissimilar filler metal that makes $T_{LW} > T_{LB}$ (Mechanism 4). A — Phase diagram; B — longitudinal cross section of weld pool.

near the fusion boundary where mixing is most limited and C_W near the bulk weld pool where mixing is complete. Thus, the liquidus temperature of the partially mixed filler metal $T_{LF'}$ is close to T_{LF} near the fusion boundary (where $T_{LF'} << T_{LB}$) and T_{LW} near the bulk weld pool (where $T_{LF'} < T_{LB}$). Thus, $T_{LF'}$ is between T_{LF} and T_{LW}. Therefore, $T_{LF} < T_{LF'} < T_{LW} < T_{LB}$ when the filler metal makes $T_{LW} < T_{LB}$.

As shown in Fig. 2B, in the bulk weld pool the solidification front is at T_{LW} because the bulk weld pool is homogeneous at the composition of C_W (undercooling is usually negligible in most arc welding). Near the pool bottom, however, the solidification front is at $T_{LF'}$ because the filler metal is only partially mixed and the average composition is $C_{F'}$ near the pool bottom. This partially mixed filler metal solidifies into a filler-rich zone along the weld near its bottom.

A stagnant or laminar-flow layer of liquid base metal can exist along the leading portion of the weld pool boundary because of weak convection near the pool boundary as suggested by Savage (Ref. 3). According to fluid mechanics (Ref. 22), the velocity of a moving liquid is zero at a solid wall, that is, the so-called "no-slip" boundary condition for fluid flow.

Since $T_{LF'}$ is well below T_{LB}, there exists a wide region ahead of the solidification front near the pool bottom corresponding to $T_{LF'} < T < T_{LB}$, that is, cooler than T_{LB}. Thus, convection can easily carry the liquid base metal from the layer of base metal near the fusion boundary into the cooler region to freeze quickly before complete mixing occurs. The liquid base metal may break up while being carried. Consequently, partially mixed base metal can scatter as islands in the filler-rich zone. The resultant welds can show numerous islands of partially mixed base metal in the form of streaks or swirls in the filler-rich zone. The composition of the islands can be somewhere between the compositions of the base metal and the bulk weld metal depending on the extent of mixing while freezing.

Since a very thin layer of liquid base metal may still exist near the pool boundary, it can also be carried by convection into the cooler region and solidify as small peninsulas right next to the fusion boundary, as suggested by Mechanism 1. This is also shown in Fig. 2B. The remaining liquid base metal can solidify as a very thin beach.

Figure 3A shows a longitudinal macrograph at the crater end of weld Ni(b)/Cu(f), taken along the weld central plane. The weld crater was longer than the macrograph and its head was thus not included. Since the melting point of pure Ni is 1455°C, the liquidus temperature of the base metal T_{LB} was 1455°C. As shown in Table 1, the dilution was 51.4%. From Equation 1 and the compositions of the base metal and filler metal, the average weld metal composition was Cu-51.3Ni or Ni-48.7Cu. From the Ni-Cu phase diagram, the liquidus temperature of the weld metal, T_{LW}, was 1321°C. Thus, T_{LW} was below T_{LB} and the difference ($T_{LB} - T_{LW}$) was as high as 134°C (1455°–1321°C).

As shown in the macrograph in Fig. 3A,

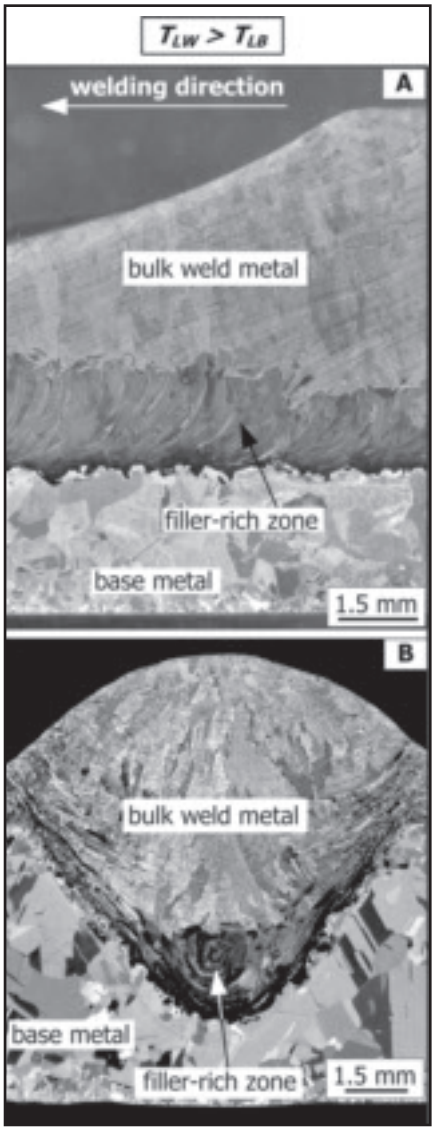

Fig. 10 — Macrographs of filler-rich zone when $T_{LW} > T_{LB}$. A — Longitudinal; B — transverse. Base metal: Cu; filler metal: Ni.

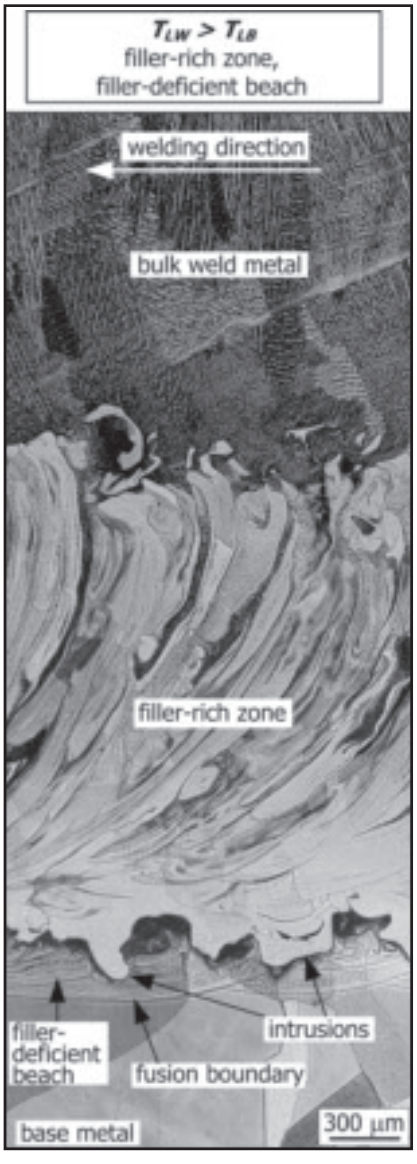

Fig. 11 — Longitudinal micrograph showing filler-rich zone formed when $T_{LW} > T_{LB}$. Base metal: Cu; filler metal: Ni.

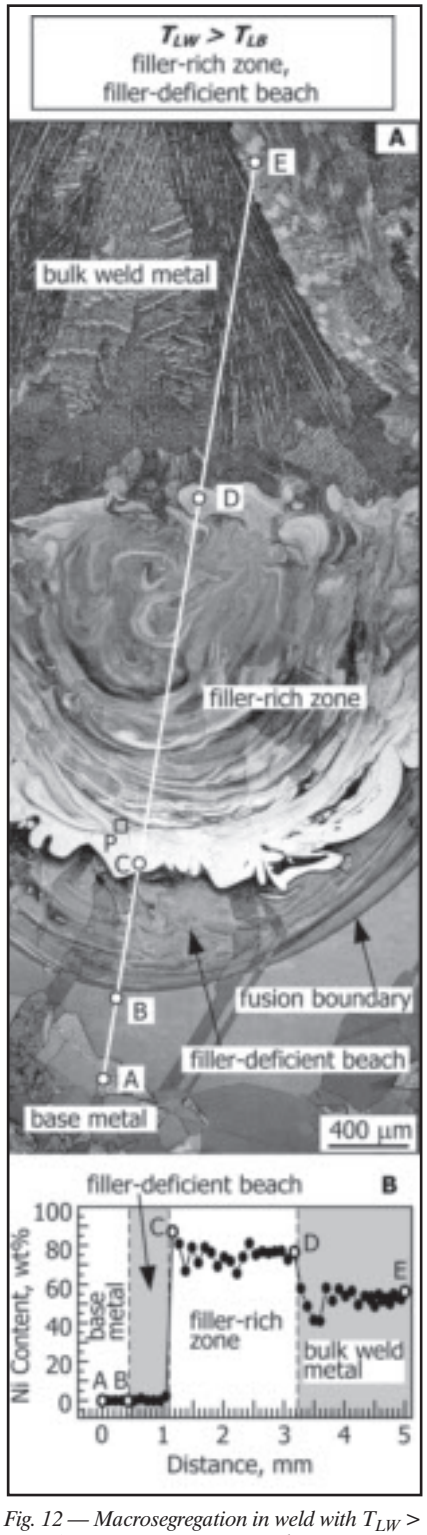

Fig. 12 — Macrosegregation in weld with $T_{LW} > T_{LB}$. A — Transverse micrograph; B — composition profile. Base metal: Cu; filler metal: Ni.

weld Ni(b)/Cu(f) is macroscopically inhomogeneous. A filler-rich zone exists along the bottom of the weld. Figure 3B shows a transverse macrograph of the same weld taken about in the middle of the weld. A filler-rich zone exists near the bottom of the weld.

Figures 4 and 5 are micrographs showing the filler-rich zone in weld Ni(b)/Cu(f). Numerous islands of partially mixed base metal exist in the filler-rich zone, some are more like streaks, and some others more like swirls. These islands were caused by weld pool convection, which can be turbulent and time dependent (Ref. 20). The darker-etching background is the filler-rich metal. A couple of small peninsulas are visible along the fusion boundary in Fig. 5. Their formation, by Mechanism 1, has been described previously (Ref. 18).

Figure 6A shows the transverse micrograph of the filler-rich zone of weld Ni(b)/Cu(f). Numerous lighter-etching islands of partially mixed base metal are surrounded by darker-etching filler-rich metal. The islands were smaller at the zone bottom but became more increasingly spread out and diffused away from it. It appears that mixing was lowest near the fusion boundary and increased away from it.

The results of macrosegregation measurements by energy dispersive spectroscopy (EDS) along path AE in Fig. 6A are shown in Fig. 6B. As shown, the weld bottom is richer in Cu (that is, the filler) than the bulk weld metal (DE) except at islands (points A, B, and C) of partially mixed base metal. This is why the area is called the filler-rich zone. The horizontal line is the average composition of the bulk weld metal of 48.7% Cu calculated based on the dilution ratio. The measured composition of the bulk weld metal fluctuates

along DE because of microsegregation across the dendrite arms. It is lower than, but still reasonably close to, the calculated one. A slightly lower value is required by the conservation of Cu because the filler-rich zone is higher than 48.7% Cu. The composition of the filler-rich metal between islands decreases from the weld bottom to the bulk weld metal, that is, from AB to BC to CD and finally DE.

The composition profile measured along path AE in Fig. 6C at smaller intervals than those in Fig. 6A is shown in Fig. 6D. The base metal AB has no Cu from the filler metal, the weld metal BC next to the fusion boundary has about 75% Cu on the average, the island CD has only about 50% Cu, and the weld metal DE just beyond the island has about 70% Cu. Thus, next to the fusion boundary (BC in Fig. 6D, where the composition of the filler-rich metal was about 75% Cu) $T_{LF'}$ = 1220°C. Thus, $T_{LF'}$ (1220°C) << T_{LB} (1445°C) near the fusion boundary.

Figure 7 shows the evidence of quick freezing of the partially mixed liquid base metal in the cooler liquid region ahead of the solidification front. Figure 7A shows the dendritic structure near point E in Fig. 6A, and Fig. 7B shows a much finer dendritic structure of island at point A in Fig. 6A. According to the composition profile shown in Fig. 6B, point E and the island at point A both have a composition of about Ni-48Cu. However, the latter has a much finer dendritic structure than the former, suggesting the latter was cooled much faster than the former — faster than what can be accounted for by the difference in location. This is consistent with the quick freezing of the partially mixed liquid base metal proposed by Mechanism 3.

Figure 8 shows the transverse macrograph of weld Ni(b)/Cu-30Ni(f). As shown in Table 1, the dilution was 38.9%. From Equation 1 and the compositions of the base metal and filler metal, the average weld metal composition was about Cu-57.4Ni or Ni-42.6Cu. From the Ni-Cu phase diagram, the corresponding liquidus temperature of the weld metal, T_{LW}, was 1342°C. Thus, T_{LW} was below T_{LB} and the difference ($T_{LB} - T_{LW}$) was as high as 113°C (1455°–1340°C).

Figure 8A shows a filler-rich zone (lighter-etching) near the bottom of weld Ni(b)/Cu-30Ni(f). This zone is somewhat smaller than that in weld Ni(b)/Cu(f) — Fig. 3B. The temperature difference ($T_{LB} - T_{LW}$) 113°C here is somewhat less than that of 134°C in the pure Ni weld made with pure Cu filler metal. As shown in the micrograph in Fig. 8B, the filler-rich zone contains many islands (light-etching) of partially mixed base metal. As compared to weld Ni(b)/Cu(f) (Fig. 6A), these islands are more like streaks than swirls.

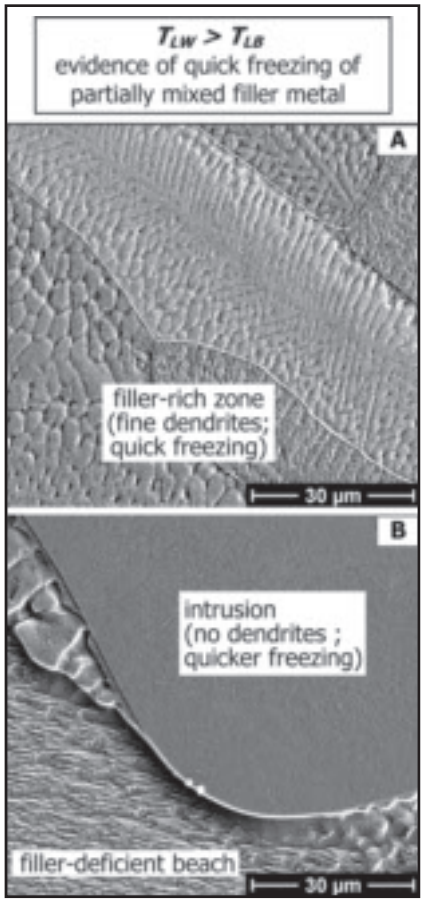

Fig. 13 — SEM images showing evidence of quick freezing of partially mixed filler metal (filler-rich liquid) in cooler layer of liquid base metal suggested by Mechanism 4. A — Filler-rich metal at point P in Fig. 12A; B — filler-rich intrusion near point C in Fig. 12A. Base metal: Cu; filler metal: Ni.

Welds with $T_{LW} > T_{LB}$

Mechanism 4, shown in Fig. 9, is for filler metals making $T_{LW} > T_{LB}$. As shown by the phase diagram in Fig. 9A, the liquidus temperature of partially mixed filler metal $T_{LF'}$ is again between T_{LF} and T_{LW}. Therefore, $T_{LF} > T_{LF'} > T_{LW} > T_{LB}$ when the filler metal makes $T_{LW} > T_{LB}$.

According to Mechanism 2 (Ref. 18), since $T_{LW} > T_{LB}$, the base metal along the outside of the T_{LW} isotherm is above its liquidus temperature T_{LB} and hence must melt completely, as shown in Fig. 9B. Thus, regardless of convection in the bulk weld pool, a stagnant or laminar-flow layer of liquid base metal must exist along the weld pool boundary. The layer solidifies into a continuous filler-deficient beach. This layer is below $T_{LF'}$ and is thus cooler than the liquid weld metal. Thus, the partially mixed filler metal pushed into this cooler layer can freeze quickly into intrusions. Filler-deficient peninsulas or islands can exist in the space formed between the intrusions in random orientation with respect to the weld interface.

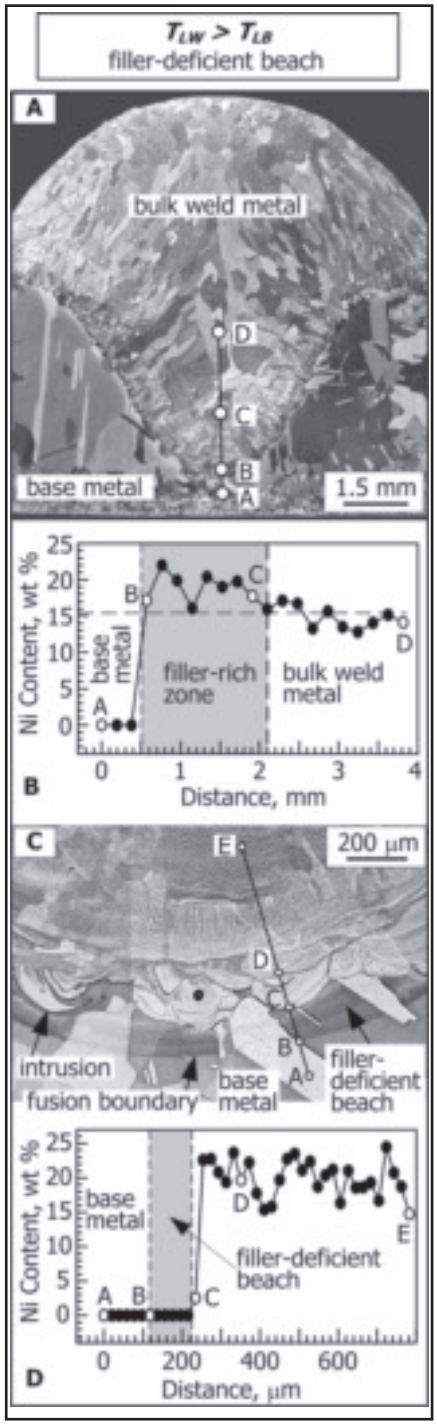

Fig. 14 — Macrosegregation in weld with $T_{LW} > T_{LB}$. A — Transverse macrograph; B — composition profile across weld bottom; C — transverse micrograph near fusion boundary; D — composition profile across fusion boundary. Base metal: Cu; filler metal: Cu-30Ni.

Since the filler metal reaches the pool bottom only partially mixed, it can freeze quickly in the region below its liquidus temperature $T_{LF'}$ near the pool bottom. This results in a filler-rich zone in the form

of a core along the bottom of the weld on the longitudinal cross section. On the transverse cross section of the weld, the filler-rich zone often appears as a filler-rich nugget. A filler-deficient beach exists between the filler-rich zone and the fusion boundary, with intrusions from the filler-rich zone.

Figure 10A shows a longitudinal macrograph at the crater end of weld Cu(b)/Ni(f)-1, taken along the weld central plane. The welding direction was from right to left. Again, the crater was longer than the macrograph and its head was thus not included. As shown, weld Cu(b)/Ni(f)-1 is macroscopically inhomogeneous. A large filler-rich zone exists along the bottom of the weld. Since the melting point of pure Cu is 1085°C, the liquidus temperature of the base metal T_{LB} was 1085°C. From Table 1, the dilution was 35.3%. From Equation 1 and the compositions of the base metal and filler metal, the weld metal composition was about Ni-35.3Cu or Cu-64.7Ni. From the Ni-Cu phase diagram, the liquidus temperature of the weld metal, T_{LW}, was 1366°C. Thus, $T_{LW} > T_{LB}$ and the difference $(T_{LW} - T_{LB})$ was as high as 281°C.

Figure 10B shows a transverse macrograph of a similar weld, that is, weld Cu(b)/Ni(f)-2 at a location well behind the crater. From Table 1, the dilution was 44.1%. From Equation 1 and the compositions of the base metal and filler metal, the weld metal composition was about Ni-44.1Cu or Cu-55.9Ni. From the Ni-Cu phase diagram, the liquidus temperature of the weld metal, T_{LW}, was 1338°C. Thus, $T_{LW} > T_{LB}$ and the difference $(T_{LW} - T_{LB})$ was as high as 253°C.

Figure 11 shows a longitudinal micrograph of the filler-rich zone well behind the crater of weld Cu(b)/Ni(f)-1. The transition from the filler-rich zone to the bulk weld metal appears rather sharp, nothing like the islands in the filler-rich zone mentioned previously. The upward and backward flow pattern of the filler-rich liquid during welding is clearly revealed. A filler-deficient beach exists along the fusion boundary between the filler-rich zone and the fusion boundary. The bottom of the filler-rich zone intrudes into the beach at various locations.

Figure 12A is a transverse micrograph of weld Cu(b)/Ni(f)-2. The light-etching, filler-rich nugget corresponds to the darker-etching band along the weld bottom in Fig. 10A and the darker-etching, filler-rich zone in Fig. 10B. A thick filler-deficient beach exists between the nugget and the fusion boundary. As shown, the bottom of the nugget extends into the filler-deficient beach of base metal as intrusions at various locations. These intrusions correspond to those shown in the longitudinal micrograph in Fig. 11. Several very small light-etching islands are also visible in the beach.

Figure 12 shows macrosegregation in weld Cu(b)/Ni(f)-2. The composition profile taken by EDS along path AE in Fig. 12A is shown in Fig. 12B. The base metal (AB at 0% Ni) is pure Cu, the beach along the fusion boundary (BC at 0% Ni) is also pure Cu, and the nugget (CD at about 75% Ni) has more Ni (that is, the filler metal) than the bulk weld metal (DE at about 52% Ni). Thus, it is clear the nugget was filler-rich and the beach was completely filler-deficient, that is, unmixed base metal (Cu). This confirms the filler-rich zone and the filler-deficient beach along the fusion boundary in the micrographs shown previously in Figs. 10 and 11. The 75% Ni of the filler-rich zone suggests that the filler-metal (originally 100% Ni) was only partially mixed before it started to freeze at a liquidus temperature of nearly 1400°C according to the phase diagram. Thus, $T_{LF'}$ (1400°C) >> T_{LB} (1085°C) near the weld bottom. The 52% Ni of the bulk weld metal was reasonably close to the 55.9% Ni average weld metal composition calculated from the dilution ratio but slightly lower. A slightly lower value is required by the conservation of Ni because the nugget already had a higher Ni content than 55.9%.

Figure 13 shows the evidence of quick freezing of the partially mixed filler metal, that is, the filler-rich liquid, in weld Cu(b)/Ni(f)-2. Figure 13A shows a fine dendritic structure at point P in Fig. 12A, thus indicating the quick freezing of the filler-rich liquid below its liquidus temperature $T_{LF'}$, as suggested by Mechanism 4. The solidification structure near point C in Fig. 12A is shown in Fig. 13B. No dendritic or even cellular structure can be seen, thus indicating an even quicker freezing of the intrusion in the cooler layer of liquid base metal along the pool boundary, as suggested by Mechanism 4. The compositions of the filler-rich metals shown in Fig. 13A and B are both about Cu-75Ni based on the composition measurement shown in Fig. 12B.

Figure 14A shows the transverse macrograph of weld Cu(b)/Cu-30Ni(f). The liquidus temperature of the base metal T_{LB} was 1085°C, the melting point of Cu. From Table 1, the dilution was 49.1%. From Equation 1 and the compositions of the base metal and filler metal, the weld metal composition was about Ni-84.7Cu or Cu-15.3Ni. From the Ni-Cu phase diagram, the liquidus temperature of the weld metal, T_{LW}, was 1168°C. Thus, $T_{LW} > T_{LB}$ and the difference $(T_{LW} - T_{LB})$ was 83°C.

The composition profile along path AD in Fig. 14A is shown in Fig. 14B. The horizontal line shows the average 15.3% Ni content of the whole weld calculated based on the dilution ratio and the compositions of the base and filler metals. Although the composition fluctuated due to microsegregation, it still can be seen that the Cu content decreases from above the average value near the weld interface to below it in the bulk weld metal. This indicates the weld bottom was richer in filler-metal than average up to around point C, although a clear filler-rich nugget could not be seen in the weld macrograph.

The filler-deficient beach and the intrusions from the weld metal are still clearly visible, as shown in the transverse micrograph in Fig. 14C. The beach is significantly thinner than that of weld Cu(b)/Ni(f)-2 in Fig. 12A. This is mainly because of the much smaller temperature difference $(T_{LW} - T_{LB})$, that is, 83°C as opposed to 253°C in weld Cu(b)/Ni(f)-2.

The composition profile along path AE in Fig. 14C is shown in Fig. 14D. The filler-deficient beach BC has no Ni and is thus completely filler-deficient or unmixed. Along CE the composition fluctuates due to microsegregation and the average is around 20% Ni, which is higher than the calculated 15.3% Cu average of the entire weld. Thus, again the weld metal near the weld bottom is richer in filler-metal than average.

For both Mechanisms 1 and 2, a filler metal with a large difference from the base metal in the liquidus temperature is more likely to cause more macrosegregation under identical welding conditions. The wire feed rate and the travel speed are likely to affect the extent of macrosegregation as well, but more work will be needed to determine their effect. The liquid viscosity and diffusion coefficient may also have some influence.

Conclusions

The present study builds upon the solidification concepts and macrosegregation mechanisms (Mechanisms 1 and 2) proposed and verified recently by the authors (Refs. 18, 19). The solidification concepts still apply here, but the macrosegregation mechanisms are more complicated because the filler metal can reach the weld pool bottom before mixing completely with the bulk weld pool and cause macrosegregation near the weld bottom. The liquidus temperatures of the bulk weld metal T_{LW}, base metal T_{LB}, filler metal T_{LF}, and partially mixed filler metal near the pool bottom $T_{LF'}$ were all considered in addition to the stagnant or laminar-flow layer of liquid base metal along the weld pool boundary suggested by Savage (Ref. 3). To verify the mechanisms the Ni-Cu binary alloy system was

selected and gas metal arc welding was conducted with dissimilar filler metals. The microstructure and macrosegregation in the resultant welds were examined. The conclusions are as follows:

1. Filler metals with a large difference from the base metal in the liquidus temperature can mix partially with the bulk weld pool during welding and cause severe macrosegregation in the bottom of the resultant weld.

2. Two new mechanisms have been proposed for the formation of macrosegregation in arc welds made with dissimilar filler metals that are not mixed with the bulk weld pool completely before reaching the pool bottom. The mechanisms, Mechanisms 3 and 4, explain the formation of two distinctly different forms of severe macrosegregation near the weld bottom well within the fusion boundary.

3. Mechanism 3 is for filler metals that lower the liquidus temperature of the weld metal, that is, $T_{LW} < T_{LB}$. Here, $T_{LF} < T_{LF'} < T_{LW} < T_{LB}$. The partially mixed filler metal forms a filler-rich liquid near the pool bottom, which solidifies at $T_{LF'}$ into a filler-rich zone along the resultant weld. Since the solidification front near the pool bottom is at $T_{LF'}$ and since $T_{LF'}$ is well below T_{LB}, there exists ahead of the front a wide region between T_{LB} and $T_{LF'}$, that is, cooler than T_{LB}. Convection can thus easily carry the liquid base metal from the stagnant or laminar-flow layer into the cooler region and allow it to freeze quickly before complete mixing occurs. This can result in numerous islands of partially mixed base metal in a filler-rich zone along the weld near its bottom.

4. A filler-rich zone has been observed near the bottom of welds made by welding Ni with filler metals Cu (T_{LW} = 1321°C and T_{LB} = 1455°C) and Cu-30Ni (T_{LW} = 1342°C and T_{LB} = 1455°C), where $T_{LW} < T_{LB}$. Islands of partially mixed base metal in the form of streaks or swirls scattered near the weld bottom well within the fusion boundary. The dendritic structure was much finer in an island near the fusion boundary than in the bulk weld metal, suggesting quick freezing of the partially mixed liquid base metal in the cooler liquid region ahead of the solidification front near the weld pool bottom. These experimental results confirm Mechanism 3.

5. Mechanism 4 is for filler metals that raise the liquidus temperature of the weld metal, that is, $T_{LW} > T_{LB}$. Here, $T_{LF} > T_{LF'} > T_{LW} > T_{LB}$. The partially mixed filler metal forms a filler-rich liquid near the pool bottom, which freezes quickly in the region cooler than $T_{LF'}$ and results in a filler-rich zone along the weld near its bottom. The stagnant or laminar-flow layer of liquid base metal solidifies as a continuous filler-deficient beach between the filler-rich zone and the fusion boundary, with filler-rich intrusions penetrating into the beach.

6. A filler-rich zone has been observed near the bottom of a weld made by welding Cu with filler metal Ni (T_{LW} = 1366°C and T_{LB} = 1085°C) and a similar weld (T_{LW} = 1338°C and T_{LB} = 1085°C), where $T_{LW} > T_{LB}$. In the transverse macrograph the filler-rich zone appeared as a nugget near the weld bottom. A filler-deficient beach existed in between the filler-rich zone and the fusion boundary with intrusions from the filler-rich zone. The absence of a discernable dendritic or cellular structure in the filler-rich intrusion suggests very quick freezing of the partially mixed filler metal in the cooler layer of liquid base metal along the pool boundary. These experimental results confirm Mechanism 4.

7. Similar but less macrosegregation has been observed in the transverse macrograph of a weld made by welding Cu with filler metal Cu-30Ni (T_{LW} = 1168°C and T_{LB} = 1085°C), where $T_{LW} > T_{LB}$ again but with a much smaller difference. These results also confirm Mechanism 4.

8. The binary Ni-Cu system is useful for studying macrosegregation in welds made with dissimilar filler metals. Its simple isomorphous phase diagram extending over a wide liquidus-temperature range of 370°C allows dissimilar-filler welds to be made with T_{LW} differing from T_{LB} to various extents.

Acknowledgments

This work was supported by the National Science Foundation under Grant No. DMR-0455484. The authors are grateful to Bruce Albrecht and Todd Holverson of Miller Electric Manufacturing Co., Appleton, Wis., for donating the welding equipment (including Invision 456P power source, and XR-M wire feeder and gun).

References

1. Houldcroft, R. T. 1954. Dilution and uniformity in aluminum alloy weld beads. *British Welding Journal* 1: 468–472.

2. Savage, W. F., and Szekeres, E. S. 1967. A mechanism for crack formation in HY-80 steel weldments. *Welding Journal* 46: 94-s to 96-s.

3. Savage, W. F., Nippes, E. F., and Szekeres, E. S. 1976. A study of fusion boundary phenomena in a low alloy steel. *Welding Journal* 55: 260-s to 268-s.

4. Duvall, D. S., and Owczarski, W. A. 1968. Fusion-line composition gradients in an arc-welded alloy. *Welding Journal* 47: 115-s to 120-s.

5. Karjalainen, L. P. 1979. Weld fusion boundary structures in aluminum and Al-Zn-Mg alloy. *Z. Metallkde* 70: 686–689.

6. Doody, T. 1992. Intermediate mixed zones in dissimilar metal welds for sour service. *Welding Journal* 61: 55–60.

7. Omar, A. A. 1998. Effects of welding parameters on hard zone formation at dissimilar metal welds. *Welding Journal* 67: 86-s to 93-s.

8. Lippold, J. C., and Savage, W. F. 1980. Solidification of austenitic stainless steel weldments: Part 2 — The effect of alloy composition on ferrite morphology. *Welding Journal* 59: 48-s to 58-s.

9. Baeslack III, W. A., Lippold, J. C., and Savage, W. F. 1979. Unmixed zone formation in austenitic stainless steel weldments. *Welding Journal* 58: 168-s to 176-s.

10. Ornath, F., Soudry, J., Weiss, B. Z., and Minkoff, I. 1991. Weld pool segregation during the welding of low alloy steels with austenitic electrodes. *Welding Journal* 60: 227-s to 230-s.

11. Albert, S. K., Gills, T. P. S., Tyagi, A. K., Mannan, S. L., Kulkarni, S. D., and Rodriguez, P. 1997. Soft zone formation in dissimilar welds between two Cr-Mo steels. *Welding Journal* 66: 135-s to 142-s.

12. Linnert, G. E. 1967. *Welding Metallurgy*, vol. 2. American Welding Society, Miami, Fla.

13. Savage, W. F., Nippes, E. F., and Szekeres, E. S. 1976. Hydrogen induced cold cracking in a low alloy steel. *Welding Journal* 55: 276-s to 283-s.

14. Rowe, M. D., Nelson, T. W., and Lippold, J. C. 1999. Hydrogen-induced cracking along the fusion boundary of dissimilar metal welds. *Welding Journal* 78: 31-s to 37-s.

15. Kent, K. G. 1970. Weldable Al-Zn-Mg alloys. *Metals and Materials* 4: 429–440.

16. Cordier, H., Schippers, M., and Polmear, I. 1977. Microstructure and intercrystalline fracture in a weldable aluminum-zinc-magnesium alloy. *Z. Metallkde* 68: 280–284.

17. Pirner, M., and Bichsel, H. 1975. Corrosion resistance of welded joints in AlZnMg. *Metall* 29: 275–280.

18. Kou, S., and Yang, Y. K. 2007. Fusion-boundary macrosegregation in dissimilar-filler welds. *Welding Journal* 86(10): 303-s to 312-s.

19. Yang, Y. K., and Kou, S. 2007. Fusion-boundary macrosegregation in dissimilar-filler Al-Cu welds. *Welding Journal* 86(11): 331-s to 339-s.

20. Kou, S. 2003. *Welding Metallurgy*, 2nd ed. Wiley, New York, N.Y., pp. 114, 180, 206, and 306.

21. ASM Int'l. 1986. *Binary Alloy Phase Diagrams, vol. 1*. ASM Int'l, Metals Park, Ohio, p. 106.

22. Kou, S. 1996. *Transport Phenomena and Materials Processing*. John Wiley and Sons, New York, N.Y., pp. 57–60.